Ecological Modelling 430 (2020) 109128

Contents lists available at ScienceDirect

Ecological Modelling

journal homepage: www.elsevier.com/locate/ecolmodel

Sensitivity of Vegetation Growth to Precipitation in a Typical Afforestation Area in the Loess Plateau: Plant-Water Coupled Modelling

Dandan Wu (Investigation; Methodology; Data analysis; Visualization; Writing - Original Draft)[a], Xianhong Xie (Resources; Writing - Review & Editing; Supervision)[b,*], Juxiu Tong (Writing - Review & Editing)[a], Shanshan Meng (Writing -Review & Editing)[b], Yibing Wang (Writing-Review & Editing)[b]

[a] School of Water Resources and Environment, China University of Geosciences, Beijing 100083, China
[b] State Key Laboratory of Remote Sensing Science, Faculty of Geographical Science, Beijing Normal University, Beijing 100875, China

ARTICLE INFO

Keywords:
Loess Plateau
Vegetation Growth
Drought
Leaf Area Index
SWAT Model
Afforestation

ABSTRACT

Vegetation dynamics are generally restricted by climate and the related soil-water state; however, the responses of vegetation growth to precipitation conditions following afforestation at a watershed scale remain unclear. In this study, we selected a typical small watershed in a semi-humid-arid transition climate zone, the Loess Plateau in China, where several afforestation programs have been implemented. We employed a plant-water coupled model to investigate the sensitivity of vegetation growth to precipitation input and to identify the effect of drought on vegetation growth during juvenile and mature stages. The model presents a favourable performance in simulating the water balance and vegetation dynamics during 2000–2015. The model and remote sensing retrieved leaf area index (LAI) produce consistent trends regarding vegetation growth. Vegetation growth is not considerably restricted by the current precipitation conditions (semi-humid); however, the growth rate may be quite sensitive to low precipitation input (semi-arid conditions), particularly in the juvenile stage following afforestation. Moreover, vegetation growth is limited by the occurrence of drought in this area. Drought events impose a lag effect on the LAI, and there may be a longer lag effect in the juvenile stage than in the mature sage. The findings from this study provide comprehensive insights into analysing vegetation responses to precipitation, with considerable implications for the implementation of ecological restoration programs in China.

1. Introduction

Vegetation plays key roles in energy, water, and carbon cycles in terrestrial ecosystems (Nemani et al., 2003; Pielke et al., 2003; Wu et al., 2016; Yuan et al., 2018; Zeng et al., 2018; Yao et al., 2019). Vegetation dynamics (including vegetation growth) is affected by both positive and negative effects of climate change, and impose strong climate feedbacks by regulating water and energy exchanges and atmospheric CO_2 concentrations (Wu et al., 2016; Green et al., 2017; Wei et al., 2017; Zeng et al., 2018). Moreover, vegetation dynamics are affected by afforestation activities in many areas of the world, such as in southern Ireland (humid climate), the Mulde basin in Germany (semi-humid climate), the Sahara (arid climate), and the Kubuqi Desert in Inner Mongolia (arid climate) (Kemena et al., 2017; Lautenbach et al., 2017; Jovani-Sancho et al., 2018; Odoulami et al., 2018; Wang et al., 2018). Due to serious soil erosion and frequent natural disasters, specifically the Loess Plateau in China is a characteristic fragile ecological area (Sun et al., 2015; Li, 2016; Wang, 2016; Jia et al., 2017; Chen, 2018). Since 1999, several reforestation programs (e.g., Grain for Green) implemented in this area have significantly improved vegetation coverage (Xie et al., 2015b; Wang et al., 2017). Therefore, it is necessary to understand the relationship between vegetation growth and climatic conditions, especially in water-limited regions.

The effect of precipitation change on vegetation growth has attracted extensive attention. A few studies employed remote sensing-based vegetation indexes, e.g., the Normalised Difference Vegetation Index (NDVI), to represent vegetation growth conditions and concluded that NDVIs are positively and strongly correlated with precipitation dynamics (Jiang et al., 2017; Tang et al., 2017; Workie and Debella, 2018; Chu et al., 2019). A similar relationship was also revealed in the Loess Plateau (Zhao, 2012; Xie et al., 2015a; Wang, 2016;

* Corresponding Author. Tel.: +861058804252.
E-mail address: xianhong@bnu.edu.cn (X. Xie).

https://doi.org/10.1016/j.ecolmodel.2020.109128
Received 11 February 2020; Received in revised form 9 May 2020; Accepted 11 May 2020

Yue et al., 2019). However, these studies have failed to fully understand the impact of precipitation on different vegetation growth stages after afforestation (e.g., the juvenile and the mature stage). Moreover, few studies considered the lag effect of interannual precipitation anomalies (especially under drought conditions) on vegetation growth, which is essential to understand the mechanisms underlying ecosystem behaviours and activities (Cao and Woodward, 1998).

To quantify the relationship between vegetation growth and precipitation dynamics, a few methods have been proposed. The most common method is the observation-based statistical regression model (Green et al., 2017; Tang et al., 2017; Chen et al., 2018; Mo et al., 2019). This black-box type of model has been widely used to identify the relationship between vegetation activity and water conditions (Wu et al., 2014), but it has limitations in parameterizing vegetation physiology, which is essential to capture the complex interactions between plant and water constraints. Alternatively, ecohydrological models that couple plant growth and water distribution are valuable for many applications. As a typical plant-water coupled model, the Soil and Water Assessment Tool (SWAT) model has been demonstrated as an effective tool for hydrological modelling and plant growth across various scales (Arnold et al., 1999; Gassman et al., 2007; Krysanova and White, 2015; Yu et al., 2017).

In this study, we aimed to understand the relationship between vegetation growth and precipitation conditions. We selected a typical watershed, the Xiuyan River watershed in a semi-humid-arid transition climate zone, which has been one of the first areas in which afforestation programs have been implemented (i.e., the Grain for Green program). We investigated two main issues:

1) What is the sensitivity of vegetation growth to precipitation change in different growth stages?
2) What is the drought lag effect on vegetation growth?

Following model evaluation on water and vegetation growth, the SWAT model was used to simulate plant-water coupled processes. This study has implications for afforestation design and management in semi-arid and semi-humid climatic conditions.

2. Data and Methods

2.1. Study Area

The study area, the Xiuyan River watershed, is located in Zichang County, Yan'an City, Shaanxi Province of the Loess Plateau, which lies between 37°1′-37°19′ N–109°12′-109°43′E, with an area of 892.4 km^2 (Fig. 1). It has a warm continental monsoon climate with a mean temperature of approximately 13°C. During the past three decades, the mean annual precipitation has been approximately 500 mm, and annual precipitation has varied from 0.6 to 1.6 times of the mean value (between approximately 300–800 mm). More than 70% of the rainfall occurs from May to September. Hence, this area is in a semi-humid-arid transition zone, with evapotranspiration accounting for about 80% of the precipitation.

The area is dominated by cropland and grassland, followed by forest, with small proportions of water and construction land. The main tree species in the forests are *Robinia pseudoacacia* and *Pinus tabulaeformis* (Yu et al., 2019). After the Grain for Green program had been implemented in the year 1999 (Zhou et al., 2009; Li et al., 2010), the proportion of forest increased from 9.02% (81 km^2) in 1990 to 21.41% (185 km^2) in 2010 (Fig. 2). Correspondingly, cropland and grassland decreased by 9.08% (86 km^2) and 3.55% (31 km^2) respectively, which implies that the afforestation project contributed a great deal to land-use change in this area. Since afforestation was implemented in plateau and hilly areas, precipitation is the only water input to the local ecosystem (Feng et al., 2016). Vegetation growth is particularly sensitive to precipitation changes (Shen et al., 2011), thus, this is an ideal area to identify the impact of precipitation on vegetation growth.

2.2. Data Availability

The SWAT model requires a Digital Elevation Model (DEM), land use, soil, and meteorological data to simulate different hydrological processes. The DEM data with a 90-m spatial resolution was obtained from the Shuttle Radar Topographic Mission (SRTM) (http://www.gscloud.cn/). Land-use maps were obtained from Remote Sensing Monitoring Data of Land Use in China (Liu et al., 2010) (http://www.resdc.cn/), and land-use data were classified into five classes, i.e., crop, forest, grass, water body, and building area. Information on soil types was collected from the Spatial Distribution Data of Soil Types in China (http://westdc.westgis.ac.cn/). Related soil physical properties were derived from the Harmonized World Soil Database (HWSD) (Nachtergaele et al., 2012; Choi et al., 2016), which combines existing regional and national properties of soil information worldwide. Soil chemical properties were calculated based on data of soil physical properties. Daily precipitation, minimum/maximum temperature, solar radiation, and average humidity data for 1980 to 2018 were acquired from the China Meteorological Administration (CMA) (http://data.cma.cn/site/index.html).

The coupled modelling was evaluated based on streamflow and the leaf area index (LAI). Daily streamflow data for the Zichang station at the watershed outlet were from the Hydrological Data of the Yellow River Basin of Hydrological Yearbook. The LAI data with an 8-day temporal resolution for 2000–2017 were obtained from a Global Land Surface Satellite (GLASS) product (Xiao et al., 2016; Xiao et al., 2017) (http://www.geodata.cn/). Table 1 presents detailed information about these data.

2.3. Model Description

SWAT is a semi-distributed, processed-based ecohydrological model (Arnold et al., 2010; Arnold et al., 2012; Bonuma et al., 2013; Tan et al., 2019). It is parameterized to simulate plant growth processes with water, temperature, and nutrient constrains. In the SWAT framework, the water balance is the basic process driving other ecohydrological processes. The water balance equation is expressed as:

$$SW_t = SW_0 + \sum_{i=1}^{t} (R_{day} - Q_{surf} - E_a - W_{seep} - Q_{gw}), \quad (1)$$

where SW_t is the final soil water content (mm H_2O), SW_0 is the initial soil water content on day i (mm H_2O), t is the time (days), R_{day} is the amount of precipitation on day i (mm H_2O), Q_{surf} is the amount of surface runoff on day i (mm H_2O), $E_a$is the amount of evapotranspiration on day i (mm H_2O), W_{seep} is the amount of water entering the vadose zone from the soil profile on day i (mm H_2O), and Q_{gw} is the amount of return flow on day i (mm H_2O).

SWAT has been coupled with a plant growth model to simulate various vegetation dynamics (Arnold et al., 1999). The model can differentiate between annual and perennial plants. In this study, we used the amount of canopy cover to indicate the condition of vegetation growth. The amount of canopy cover is expressed as the LAI, which is defined as the area of green leaves per unit area of land. Under ideal growing conditions, for perennials, the leaf area added on day i is calculated using the following equation:

$$\Delta LAI_i = (fr_{LAImx,i} - fr_{LAImx,i-1}) \cdot \left(\frac{yr_{cur}}{yr_{fulldev}}\right) \cdot LAI_{mx} \cdot (1 - \exp(5 \cdot \left(LAI_{i-1} - \left(\frac{yr_{cur}}{yr_{fulldev}}\right) LAI_{mx}\right))), \quad (2)$$

The accumulated LAI is expressed as:

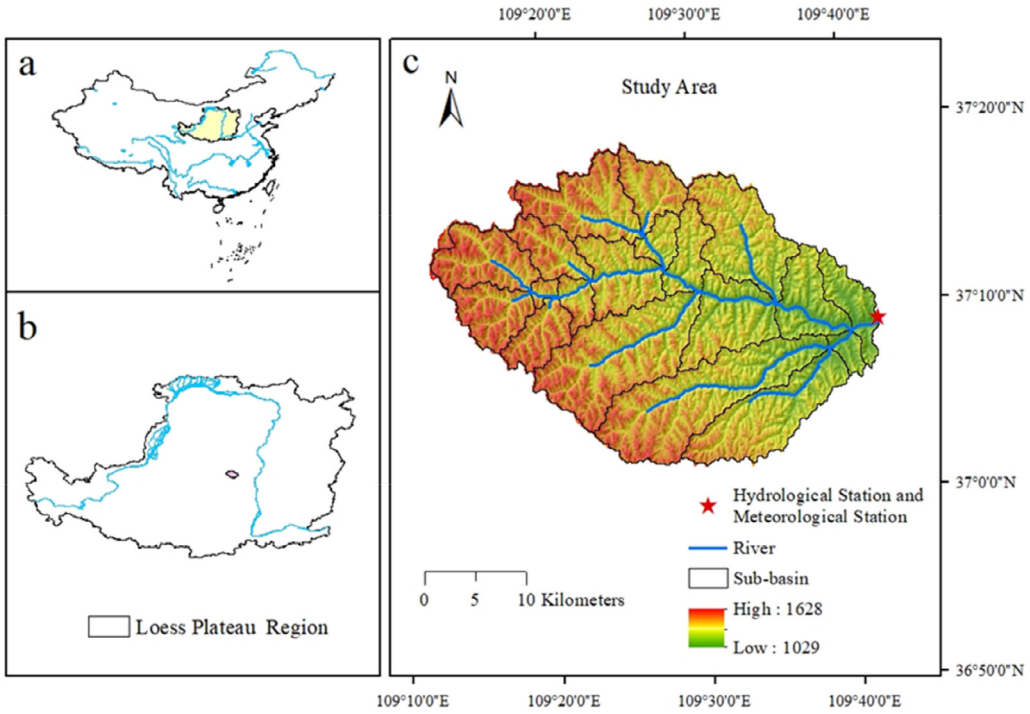

Fig. 1. China's regional boundary (a), Loess Plateau boundary and location of the study area (b), location of the river and China Meteorological Administration (CMA) station and hydrological station (c).

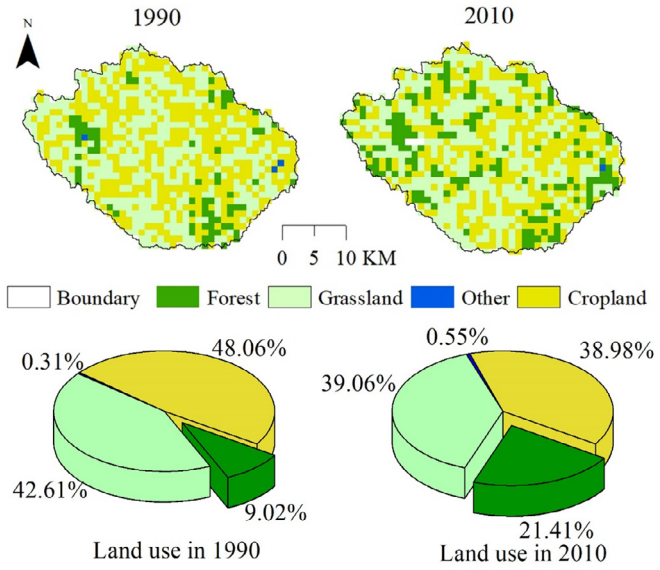

Fig. 2. Land use change from 1990 to 2010 in the Xiuyan River watershed.

$$LAI_i = LAI_{i-1} + \Delta LAI_i, \tag{3}$$

where ΔLAI_i is the leaf area added on day i, LAI_i and LAI_{i-1} are the leaf area indices for day i and i-1, respectively, $fr_{LAImx,\ i}$ and $fr_{LAImx,i-1}$ are the fraction of the plant's maximum LAI for day i and i-1, LAI_{mx} is the maximum LAI for the plant, yr_{cur} is the age of the tree (years), and $yr_{fulldev}$ is the number of years for the tree species to reach full development (years). According to equation 2, the model employs different vegetation growth modes for the juvenile and the mature stages. For the juvenile stage ($yr_{cur} < yr_{fulldev}$), the accumulated LAI will vary depending on the age of the tree relative to the number of years required for the tree to mature. For the mature stage ($yr_{cur} \geq yr_{fulldev}$), the accumulated LAI will not depend on the age increase. Thus, $yr_{fulldev}$ is an important parameter for vegetation growth.

When leaf senescence becomes the dominant growth process, the LAI for perennials is calculated as:

$$LAI = \left(\frac{yr_{cur}}{yr_{fulldev}}\right) \cdot LAI_{mx} \cdot \frac{(1 - fr_{PHU})}{(1 - fr_{PHU,sen})} \; fr_{PHU} > fr_{PHU,sen}, \tag{4}$$

where LAI is the LAI for a given day, LAI_{mx} is the maximum LAI, fr_{PHU} is the fraction of potential heat unit accumulated for the plant on a given day in the growing season, $fr_{PHU,\ sen}$ is the fraction of the growing season (PHU) at which senescence becomes the dominant growth process.

Actual plant growth differs from the above potential growth due to temperature, water, and nutrient constraints. The actual leaf area added on day i is calculated as:

$$\Delta LAI_{act,i} = \Delta LAI_i \cdot \sqrt{\gamma_{reg}}, \tag{5}$$

where $\Delta LAI_{act,\ i}$ is the actual leaf area added on day i, ΔLAI_i is the potential leaf area added on day i that is calculated with equation (1) or (2), and γ_{reg} is the plant growth factor (0.0–1.0).

The plant growth factor quantifying the constraints is calculated as:

$$\gamma_{reg} = 1 - \max(wstrs,\ \ tstrs,\ \ nstrs,\ \ pstrs), \tag{6}$$

where $wstrs$ is the water stress for a given day, $tstrs$ is the temperature stress for a given day expressed as a fraction of optimal plant growth, $nstrs$ is the nitrogen stress for a given day, and $pstrs$ is the phosphorus stress for a given day.

The water stress for a given day is calculated as:

$$wstrs = 1 - \frac{E_{t,\ act}}{E_t} = 1 - \frac{w_{actualup}}{E_t}, \tag{7}$$

where E_t is the maximum plant transpiration on a given day (mm H_2O), $E_{t,\ act}$ is the actual amount of transpiration on a given day (mm H_2O), and $w_{actualup}$ is the total plant water uptake for the day (mm H_2O). In this study, we only considered the water constraint and removed nitrogen and phosphorus stress. Therefore, the scenario simulation results of the model were assumed to be only contributed by the precipitation change. Given the consideration of the water constraint, previous soil

Table 1
Data descriptions and sources used.

Data type	Resolution	Database name	Source
Digital Elevation Model (DEM)	90 m	SRTMDEM 90M Resolution Raw Elevation Data	GS Cloud (http://www.gscloud.cn/)
Soil type	1 km	Spatial Distribution Data of Soil Types in China	Resource and Environment Data Cloud Platform (http://www.resdc.cn/)
Land use	1 km (1990, 2010)	Remote Sensing Monitoring Data of Land Use in China	Resource and Environment Data Cloud Platform (http://www.resdc.cn/)
Meteorological data	Daily (1980–2017)	Annual Daily Value Data Set of Ground in China	National Meteorological Information Center (http://data.cma.cn/site/index.html)
streamflow	Daily (2006,2008–2012)	Hydrological Data of the Yellow River Basin	Annual Hydrological Report of China
Leaf area index (LAI)	1 km, 8-day (2000–2017)	GLASS Products-LAI	National Earth System Science Data Center (http://www.geodata.cn/)

water conditions (e.g., water stress during a drought) in the year due to precipitation anomalies will impact the later soil water storage, thereby affecting vegetation growth. Thus, the SWAT model with a plant-water coupled process cannot only simulate the interannual change in the LAI, but also its daily change. The plant growth in a given year will vary depending on the age of the tree and environmental conditions (e.g., water and temperature).

2.4. Model Setup, Calibration and Validation

The study area was divided into 19 sub-basins (Fig. 1), and 89 hydrologic response units (HRUs). The detailed model setup in this study is shown in Fig. 3.

The Soil and Water Assessment Tool-Calibration Uncertainty Program (SWAT-CUP) software package was used in this study for model calibration, validation, sensitivity, and uncertainty analysis (Liu et al., 2010). This package employs the Sequential Uncertainty Fitting version 2 (SUFI-2) algorithm to map all uncertainties (parameter, conceptual model, input, etc.) on the parameters (expressed as uniform distributions or ranges). It is able to capture the majority of the measured data within the 95% prediction uncertainty (95PPU) of the model in an iterative process. Three objective functions i.e., determination coefficient (R^2), Nash-Sutcliffe efficiency (NSE), and percentage Bias, were used to search for optimal parameter values.

The eco-hydrological model was calibrated and validated with respect to water balance and vegetation dynamics. For the water balance, although the soil-water state is a direct factor constraining vegetation growth, we employed streamflow as a surrogate to evaluate the model performance due to data availability (moreover, streamflow is the most widely used variable in hydrological model evaluation). According to the sensitive parameters in SWAT (Santhi et al., 2001; Muleta and Nicklow, 2005; Arabi et al., 2008; Yu et al., 2017), six parameters were selected for streamflow calibration regarding runoff generation and routing processes (Table 2).

For the calibration of vegetation related parameters, we first determined the initial value of each vegetation parameter according to the SWAT database, and then optimized the vegetation parameters of different vegetation types, so that the simulated LAI matched the GLASS LAI as well as possible. Based on the plant growth formulation, five parameters were selected for LAI calibration (Table 3).

We first calibrated the runoff related parameters (Table 2), and then the vegetation related parameters (Table 3). It may be beneficial to combine both streamflow and LAI, but it is difficult to set an objective function because of this multi-objective optimization problem. Moreover, the Soil and Water Assessment Tool-Calibration Uncertainty Program (SWAT-CUP) can only be used for runoff related parameter calibrations, while the vegetation related parameters need to be manually adjusted. Thus, we optimized the runoff- and vegetation-related parameters separately, although the two processes are actually coupled. Based on such a calibration and validation for water balance and vegetation dynamics, optimal parameter values were achieved for subsequent simulations with different scenarios.

2.5. Experiment Design

According to the precipitation condition in the study area, precipitation in this area fluctuates between 0.6 and 1.6 times the mean value. Moreover, precipitation in 2004 and 2015 was approximately 289 mm and 329 mm, respectively, i.e., well below the annual mean precipitation, which shows that drought events occurred in these two years, which may have imposed different stresses on vegetation growth.

To identify the sensitivity of vegetation growth to the precipitation dynamics and the drought events, we designed four scenarios with different precipitation conditions, as illustrated in Fig. 3. In scenario 1, for the period of 2000–2017, the precipitation input for the model was set at 0.6 times the actual precipitation. Therefore, the mean annual precipitation was approximately 312 mm, which represents a semi-arid climate condition. In scenario 2, the precipitation input was the actual time series with a mean of approximately 520 mm. This scenario indicates a semi-humid condition and can be taken as a baseline simulation, and was the scenario used for the model calibration and validation. In scenario 3, the precipitation input was set as 1.6 times the actual time series, and its value was approximately 832 mm, which represents a humid climate condition. In scenario 4, except that the precipitation input in 2004 and 2015 was the average annual precipitation, the precipitation input in the other years was the same as that in scenario 2. This scenario was designed to enable the discussion of the drought lag effect of vegetation growth. The lengths of the two stages were identified according to the temporal variation in the LAI. Since this study focused on vegetation dynamics after afforestation, the vegetation in this paper mainly refers to forest, and the simulated LAI is with respect to the forest land.

3. Results

3.1. Model Calibration and Validation

3.1.1. Streamflow

The model for the water balance simulation was calibrated for the periods of 2006 and 2008–2009 and was validated for the period of 2010–2012 with a warm-up period of 3 years (1997-1999). We used three years to spin-up the model, given that there was little afforestation practice before the year 2000. Afforestation operations in the SWAT model started at the fourth year (i.e., in 2000), which is in line with the actual situation. Fig. 4 shows the simulation results of the daily runoff for calibration and the 2010–2012 validation at Zichang station.

The simulated streamflow was consistent with the corresponding observations. The determination coefficient (R^2) was 0.70 for the calibration and 0.73 for the validation, and the NSE was up to 0.70. The bias was –1.51% for the calibration and 5.99% for the validation. The simulation results suggest that the SWAT model performance was satisfactory and acceptable according to the criteria used in this

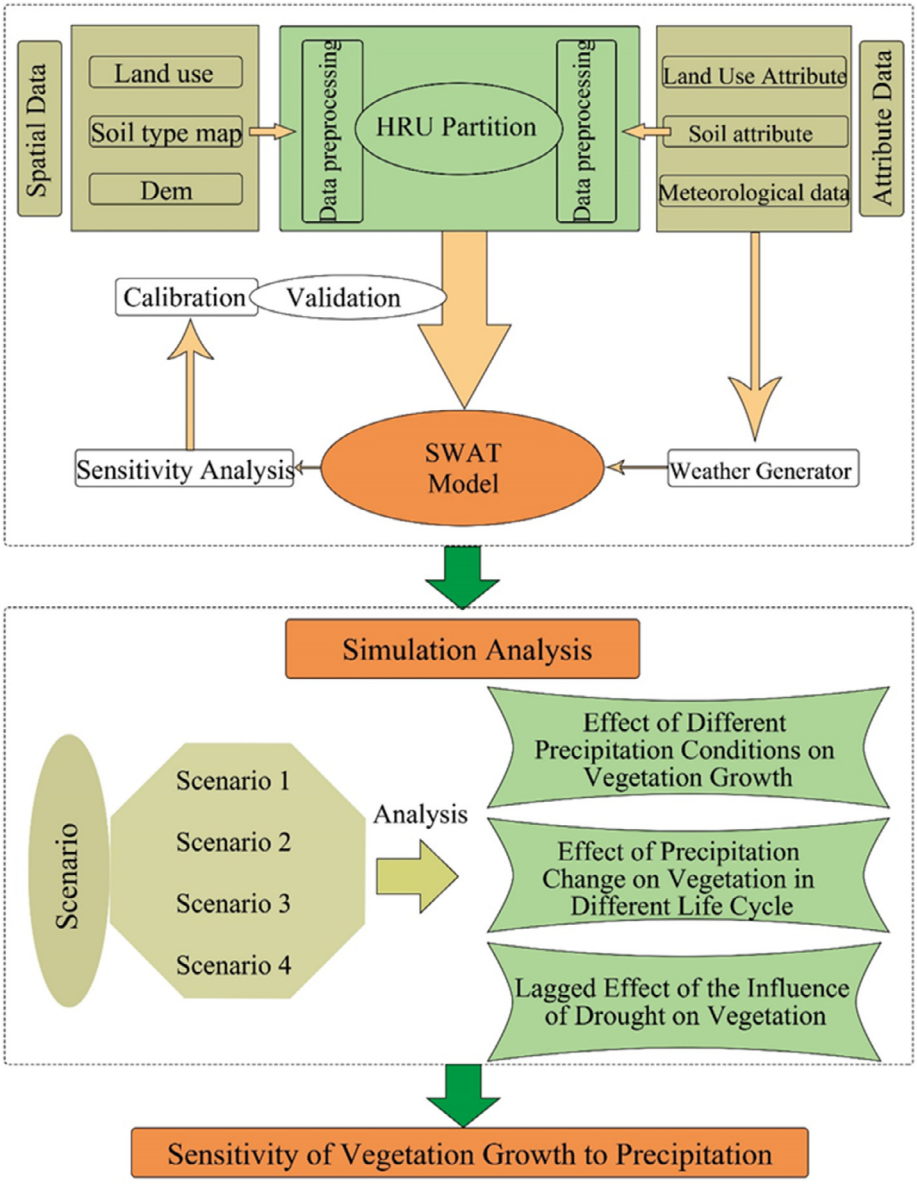

Fig. 3. Flow chart applied in this study. HRU – hydrological response unit, SWAT – soil and water assessment tool.

application (Nash and Sutcliffe, 1970). Overall, the SWAT model and related parameters were reliable to simulate the water balance in the catchment.

3.1.2. Leaf Area Index (LAI)

As the main vegetation growing season in the study area is from May to September, we selected the LAI from this growing season for calibration and validation. For forest, the increase in the LAI was related to the change in tree structure. In this study, grass is actually a perennial vegetation with mixed shrubs and grasses, not a simple annual vegetation. Thus, the LAI for the grassland should increase annually. Therefore, we validated the LAI from forest and grassland. The results of the simulated model for the forest and grassland LAIs were consistent, in terms of time, with the corresponding GLASS LAI (Fig. 5). Please note that the model and the GLASS presented a similar increase for the grass LAI because the grassland is composed of mixed perennial vegetation.

Table 4 shows the simulation results of the forest and grassland LAIs for 2000–2011 (calibration) and 2012–2017 (validation). For the forest, the determination coefficient (R^2) was 0.80 for the calibration

Table 2
Parameters used in the runoff calibration processes.

Parameter	Model input file	Description	Value range
CN_2	mgt	SCS runoff curve number	20~100
GW_DELAY	gw	Groundwater delay (days)	–10~10
GWQMN	gw	Threshold depth of water in the shallow aquifer required for return flow to occur (mm)	0~5000
CH_K2	rte	Effective hydraulic conductivity in main channel alluvium	0~150
SOL_AWC (1)	sol	Available water capacity of the soil layer	0~1
SOL_K (1)	sol	Saturated hydraulic conductivity	0~2000

Table 3
Parameters used in the leaf area index (LAI) calibration processes.

Parameter	Model input file	Description
BLAI	Plant.dat	Max leaf area index
FRGRW1	Plant.dat	Fraction of the plant growing season corresponding to the 1st. Point on the optimal leaf area development curve.
FRGRW2	Plant.dat	Fraction of the plant growing season corresponding to the 2nd. Point on the optimal leaf area development curve.
HEAT_UNITS	mgt	Total heat units for cover/plant to reach maturity
CURYR_MAT	mgt	Current age of trees (years)

and 0.85 for the validation, and the corresponding NSE values were 0.73 and 0.82, respectively. Accordingly, the calibration and validation of grassland also achieved acceptable results. Fig. 6 shows the simulated LAI and Global Land Surface Satellite (GLASS) LAI for the 19 subbasins in the study area, which were almost consistent in their spatial distribution. Given the appropriate parameterizations and the favourable performance, the model results were reliable to interpret the response of plant growth after afforestation.

3.1.3. Climate and LAI Changes

The interannual precipitation and air temperature showed different temporal variations (Fig. 7). Precipitation has had large interannual changes in this area. The amount of precipitation was > 700 mm in 2002, whereas it was only 289 mm in 2004 and 329 mm in 2015, indicating that drought events occurred in 2004 and 2015. However, the interannual temperature in the region has shown little change, with a mean of approximately 13 °C. In response to such climate conditions, the soil water in this area simulated by SWAT had similar dynamics to those of the precipitation, and it reached a low level in 2004 and 2015, about 172 mm and 134 mm, respectively.

Evidently, the performance of the simulated LAI was basically the same as that of the GLASS LAI (R^2 = 0.77, NSE = 0.71 and Bias = 4.15%), whereby both increased annually. The LAI increased from 0.34 in 2000 to 1.34 in 2017. Interestingly, the simulated LAI showed an upward trend in 2002 and a slight decrease in 2015, which was basically consistent with the precipitation and soil water fluctuation. Although the simulated LAI did not decrease in 2004, it showed a downward trend in 2005, which may be due to the lag effect of drought on the LAI. It has to be noted that the GLASS LAI also showed a lag effect in 2005, as it remained at the same level as that in 2004 (about 0.65). While the SWAT simulation failed to trace specific fluctuations in the GLASS LAI (e.g., the sharp increase in 2002), it successfully captured the general pattern of the LAI increase. According to the soil water dynamics, the lag effect in 2015 was not obvious because the water stress referring to the low level of soil moisture due to the 2015 drought was largely relaxed by the precipitation in 2016 (Fig. 7). In contrast, the 2004 drought was more severe than that in 2015, according to precipitation and soil moisture. Thus, soil moisture and the related vegetation growth state (i.e., LAI) did not recover in 2005. These analyses suggest that precipitation may have a substantial impact on vegetation dynamics. In addition, the LAI increased rapidly prior to 2012, whereas it tended to stabilise after 2012. Given the life cycle of tree species, the first 12 years were assumed as a juvenile stage, after which the vegetation was assumed to be in a mature stage. A few other studies also indicated that the tree species planted on the Loess Plateau need about 12 years to mature (Hu et al., 1992; Liu, 1998; Xu et al., 2003; Zhu et al., 2004). Therefore, we set the mature stage $yr_{fulldev}$ = 12 in the modelling and investigated the lag effect in the two stages.

The vegetation LAI also showed spatial variability (Fig. 8). In 2001, the LAI in most areas was < 0.5, especially in the northwest, where the LAI was < 0.3. In contrast, in 2017 the LAI of the entire area reached 0.9 and exceeded 1.5 in the southeast part. Generally, the LAI in the southeast of the study area was larger than that in the northwest, which was likely due to the lower elevation in the southeast and the relatively rich water resources. There was only a small difference in the LAI between 2013 and 2017 because the vegetation reached the mature stage. Moreover, the LAI in 2015 was even lower than that in 2013 due to the drought in 2015.

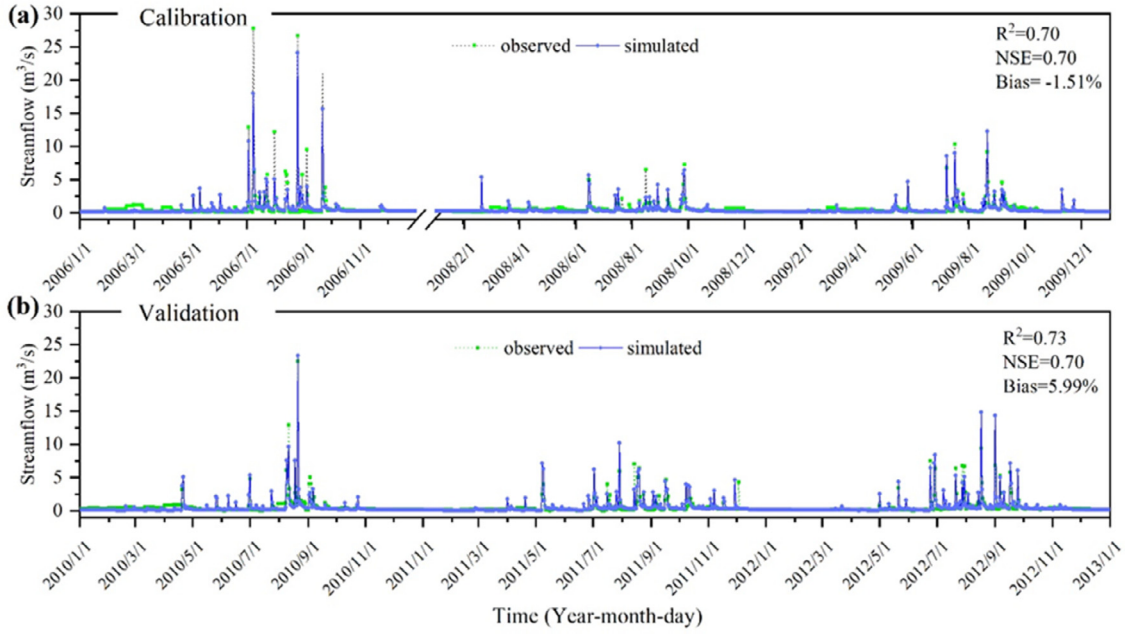

Fig. 4. (a) Calibration and (b) validation results for daily streamflow. NSE – Nash-Sutcliffe efficiency.

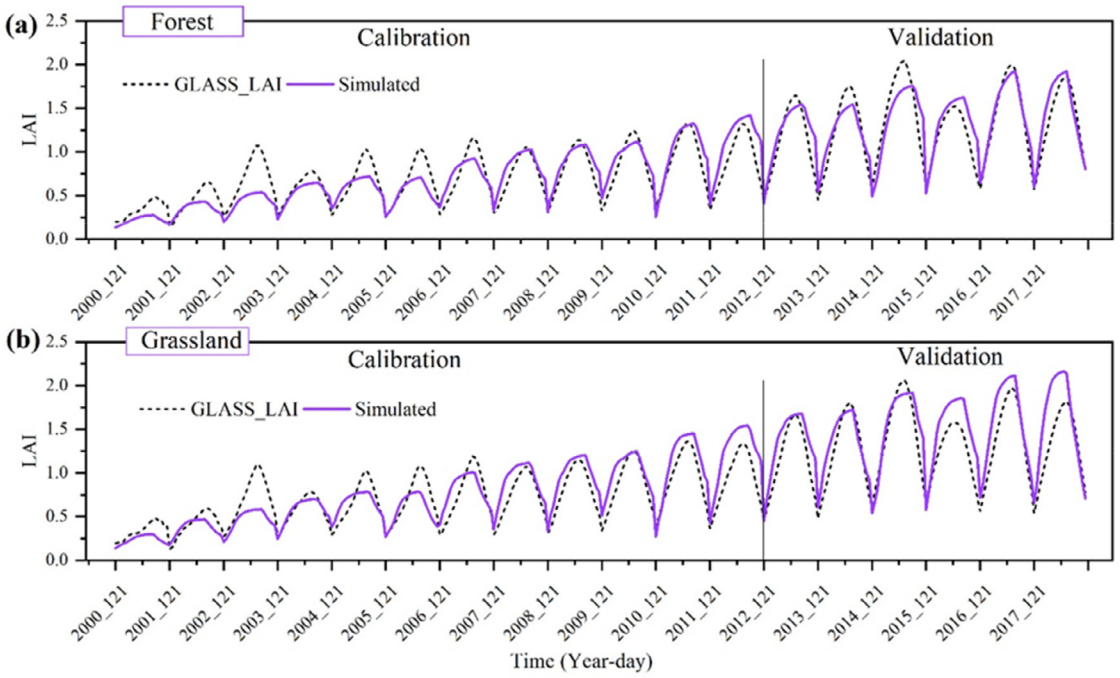

Fig. 5. Calibration and validation results for (a) forest and (b) grassland leaf area index (LAI).

Table 4
Leaf area index (LAI) calibration and verification results. NSE – Nash-Sutcliffe efficiency.

Vegetation types	Simulated period (year)	R2	NSE	Bias (%)
Forest	Calibration 2000–2011	0.80	0.73	0.61
	Verification 2012–2017	0.85	0.82	1.10
Grassland	Calibration 2000–2011	0.78	0.72	5.72
	Verification 2012–2017	0.80	0.74	2.83

3.2. Sensitivity of Vegetation Growth

3.2.1. Effect of Different Precipitation Conditions on Vegetation Growth

The simulation results of scenarios 1–3 are shown in Fig. 9 (a). It was found that the LAI from scenario 3 (1.6 P) was slightly larger than that from scenario 2 (P). The LAI from scenario 1 (0.6 P) fluctuated sharply and was considerably lower than that of scenario 2. For instance, the LAI decreased from 0.53 (scenario 2) to 0.36 (scenario 3) in 2005 and from 1.32 to 0.89, respectively, in 2015. To further examine the precipitation impact on vegetation in the modelling, we prescribed different precipitation inputs from 0.2 to 2 times (i.e., the multiplier of

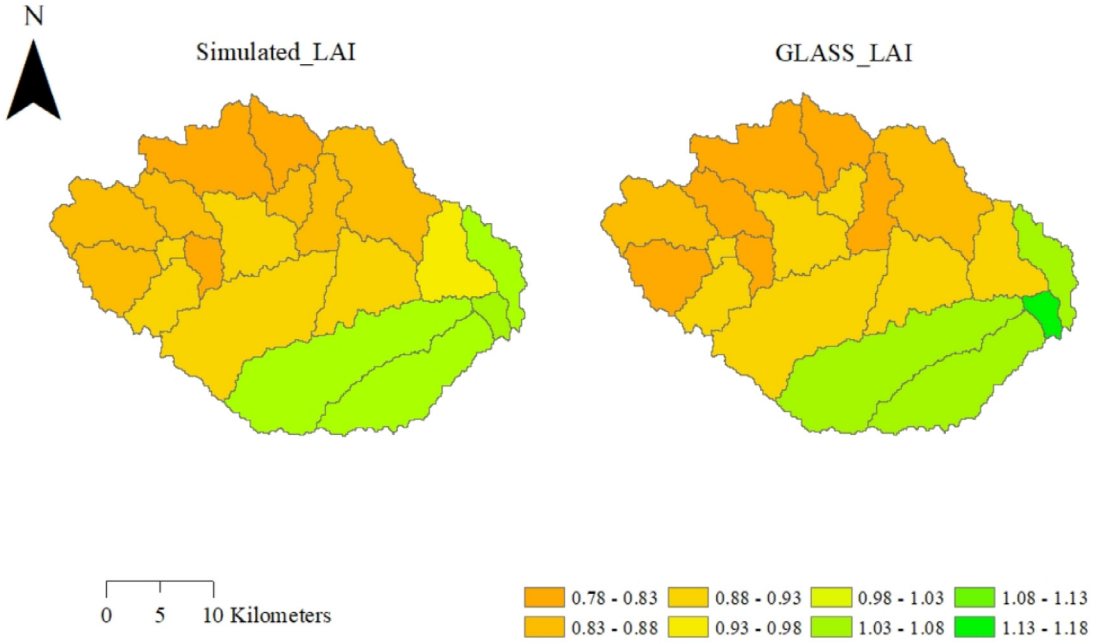

Fig. 6. Spatial distribution of the simulated LAI and Global Land Surface Satellite LAI (GLASS LAI) from April to September for 2000 to 2017 in Xiuyan River watershed, China. LAI – leaf area index.

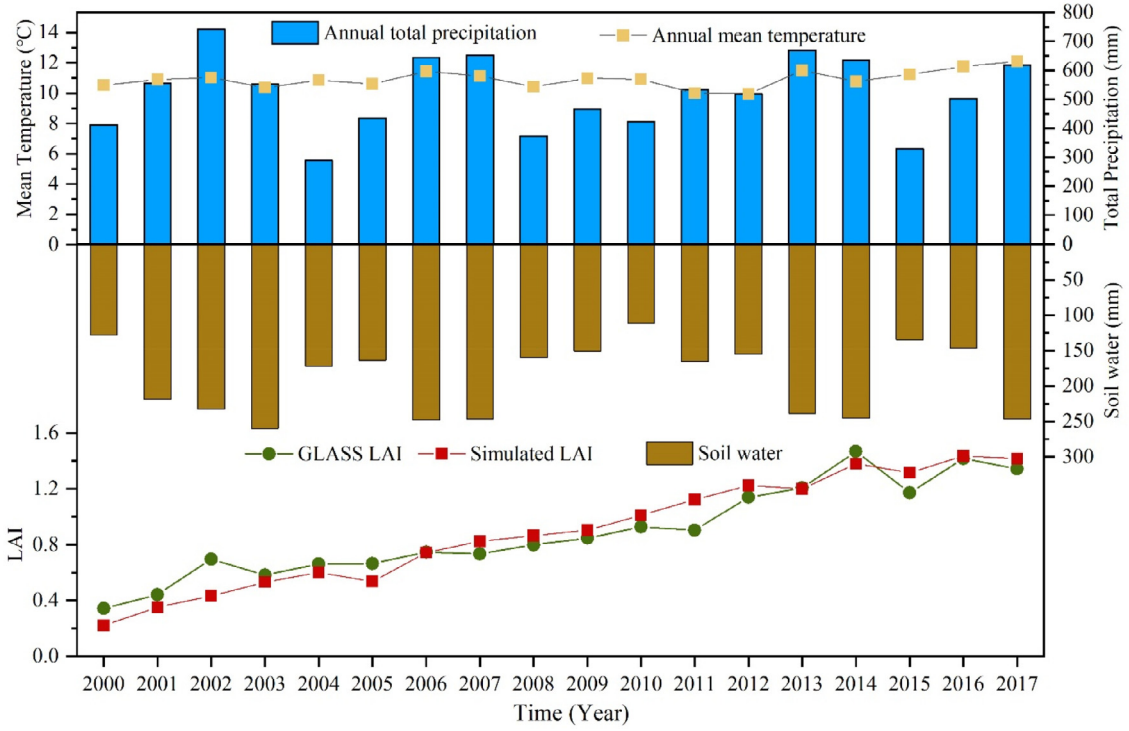

Fig. 7. Precipitation, temperature, soil water, and LAI changes from 2000 to 2017.

precipitation α in Fig. 9 c) the actual precipitation time series. Fig. 9 (b) and Fig. 9 (c) present the responses of the LAI and biomass to the precipitation conditions (the multiplier α), respectively. It is perceived that the LAI and biomass had logarithmic correlations with precipitation, as the coefficients of determination (R^2) were 0.93 and 0.86, respectively, in the fitting formulas, and with the increase of precipitation, the LAI and biomass growth rates also decreased. Beyond that, and if $\alpha < 1$, vegetation growth was more sensitive to a precipitation change, whereas if $\alpha > 1$, the sensitivity was substantially decreased.

3.2.2. *Effect of Precipitation Change on Vegetation in Different Stages of the Growth Cycle*

We identified the sensitivity of the LAI in the juvenile and the mature stages from May to September in the three scenarios (scenarios 1-3). The LAI of the mature stage was clearly greater than that of the juvenile stage in the three scenarios (Fig. 10). From May to September, the largest LAI difference between the juvenile stage and the mature stage appeared in July, while the smallest difference occurred in May. Fig. 10 (d) and 10 (e) show the LAI change rate of scenario 1 and scenario 3, respectively, relative to scenario 2. The LAI change rate in the mature stage of scenario 1 was 4% higher than that in the juvenile stage, and the highest was in June (5%). However, in scenario 3, there was no significant difference between the LAI change rate in the mature stage and the juvenile stage, especially in July and August, while the largest difference appeared in May. At the same time, the LAI change rate in the mature stage was approximately 1% higher than that in the juvenile stage.

3.3.3. *Lagged Effect of the Influence of Drought on Vegetation*

The difference (scenario 2 – scenario 4) in the LAI between scenario 2 and scenario 4 is shown in Fig. 11. The LAI in scenario 2 was 0.017 and 0.132 lower than that in scenario 4 in 2004 and 2005, respectively. Interestingly, in scenario 2, after the drought in 2004, the LAI in 2005 decreased more than in 2004, which shows that the interannual lag effect of drought on vegetation growth was significant in the juvenile stage. On the contrary, the negative anomaly of precipitation in 2015 almost only caused the LAI to decrease in that year, which shows that the hysteresis of the influence of drought on vegetation is not very significant in the mature stage. We further explored the response of the daily LAI during the two drought events. Although the negative precipitation anomaly began in May of 2004 and 2015 (Fig. 12), the negative LAI differences appeared after June of the two years. The largest absolute LAI differences were up to –0.03 and –1.7 in June for 2004 and 2015, respectively, where the largest proportional LAI difference reached –4.4% and –9.5% in late June until September. Thus, the lag effect of the two droughts is one month at least.

4. Discussion

4.1. *Impacts of Precipitation on Vegetation Growth*

This study identified the sensitivity of vegetation growth to precipitation change. The results show that vegetation growth is substantially limited by precipitation and that the sensitivity of vegetation to precipitation varies in different life stages. Drought has a lag effect on vegetation growth. Although there have been many reports on the sensitivity of vegetation growth to precipitation change, the majority were based on black-box type models with statistical regressions (Kong et al., 2017; Quetin and Swann, 2017; Tang et al., 2017; Chen et al., 2018; Li et al., 2019; Mo et al., 2019). In this study, we employed a plant-water coupled model to simulate vegetation growth. We not only clarified the specific effects of different precipitation conditions on vegetation growth, but also found that the lag effect of drought in different vegetation life cycle stages differed, which has also been revealed by other studies (Martiny et al., 2006; Mberego, 2017; Papagiannopoulou et al., 2017; Li et al., 2019; Mo et al., 2019).

We found that the trend of vegetation growth varied with the increase in precipitation within a certain range and that there was a roughly logarithmic relationship between vegetation growth and precipitation (Fig. 9). This finding has also been discussed by previous studies (Chang et al., 2014; Yang et al., 2015; Zhu et al., 2015; Justine et al., 2017; Tang et al., 2017) in which close relationships were

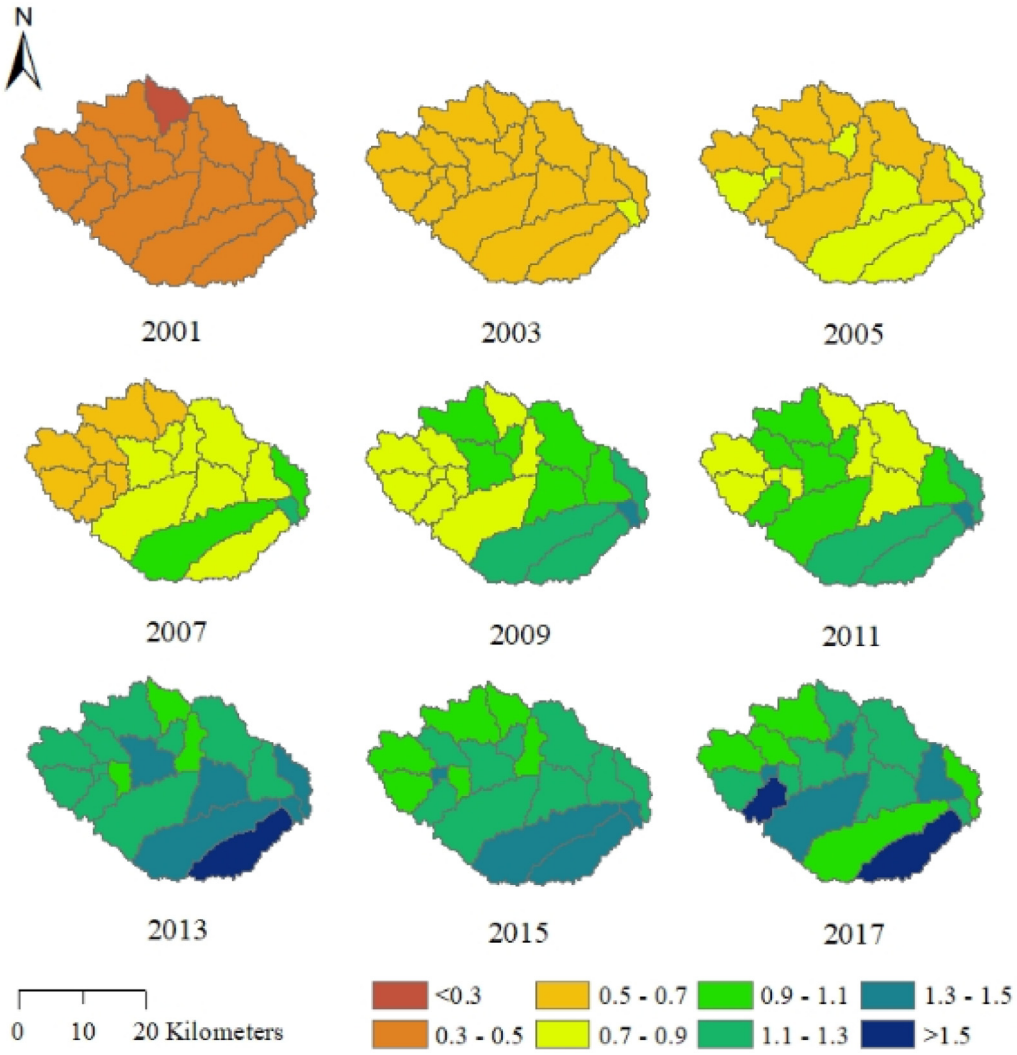

Fig. 8. Spatial distribution of the Global Land Surface Satellite (GLASS) LAI.

established between the vegetation index and climate factors. Li et al. (2019) found that a stepwise multiple regression equation can well represent the relationship between the LAI and precipitation. Del-Toro-Guerrero et al. (2019) reported that vegetation greenness showed significant temporal and spatial correlations with precipitation features. Furthermore, what is surprising is that the growth rate of LAI and biomass decreased with increasing precipitation (Fig. 9). This finding was consistent with Tang et al. (2017), who indicated that vegetation growth in a low-precipitation area was more sensitive to precipitation than that in a high-precipitation area. This implies the existence of a precipitation threshold, beyond which vegetation growth will not be limited by precipitation, but rather controlled by other factors, such as carbon dioxide, solar radiation, tree-age, etc. (Gavito et al., 2001; Juvany et al., 2013).

Our study revealed the effect of precipitation change on the vegetation in different stages of the growth cycle. When the annual precipitation was < 400 mm in scenario 1 for semi-arid climate conditions, vegetation growth in the juvenile stage was more sensitive to precipitation input than in the mature stage. In contrast, when the annual precipitation was > 400 mm in scenario 2 for semi-humid climate conditions, vegetation growth in the mature stage was more sensitive to precipitation than in the juvenile stage, although the sensitivity was not particularly distinct. This may be due to the large water demand during the maturity of the vegetation. Previous studies have investigated seasonal effects of precipitation on vegetation growth (Gaughan et al., 2012; Chen and Weber, 2014; Cramer and Hoffman, 2015; Mberego, 2017; Liu et al., 2018; Zp et al., 2018). Tang et al. (2017) explored the spatiotemporal changes of vegetation growth and the responses to climate changes and found that the summer NDVI was positively correlated with summer precipitation. In comparison to previous studies, our study not only discussed the sensitivity difference during the main growing season (May-September), but also analysed the sensitivity of vegetation in the juvenile and mature stages to the precipitation change under different climatic conditions.

Our study also found that drought had a lag effect on vegetation growth. Previous studies have independently reached the same conclusion (Martiny et al., 2006; Mberego, 2017; Papagiannopoulou et al., 2017; Tang et al., 2017; Li et al., 2019; Mo et al., 2019). Yet, in contrast to previous research, our study discovered the lag effect of drought on vegetation growth in different life cycles (juvenile and mature stages) (Fig. 12). Our study found that the lag effect of drought on vegetation growth in different life cycles (young and mature) is also different (Fig. 12). This may be because, in the juvenile stage, the increase in the LAI mainly depends on the age of the plants and the vegetation state at the end of the last year. In the mature stage, the increase in the LAI is not related to the age and the vegetation state of the previous year, but mainly relies on the climate of the current year. Therefore, the lag effect is different between the juvenile and the mature stage. There are several possible reasons for a time lag between precipitation and vegetation

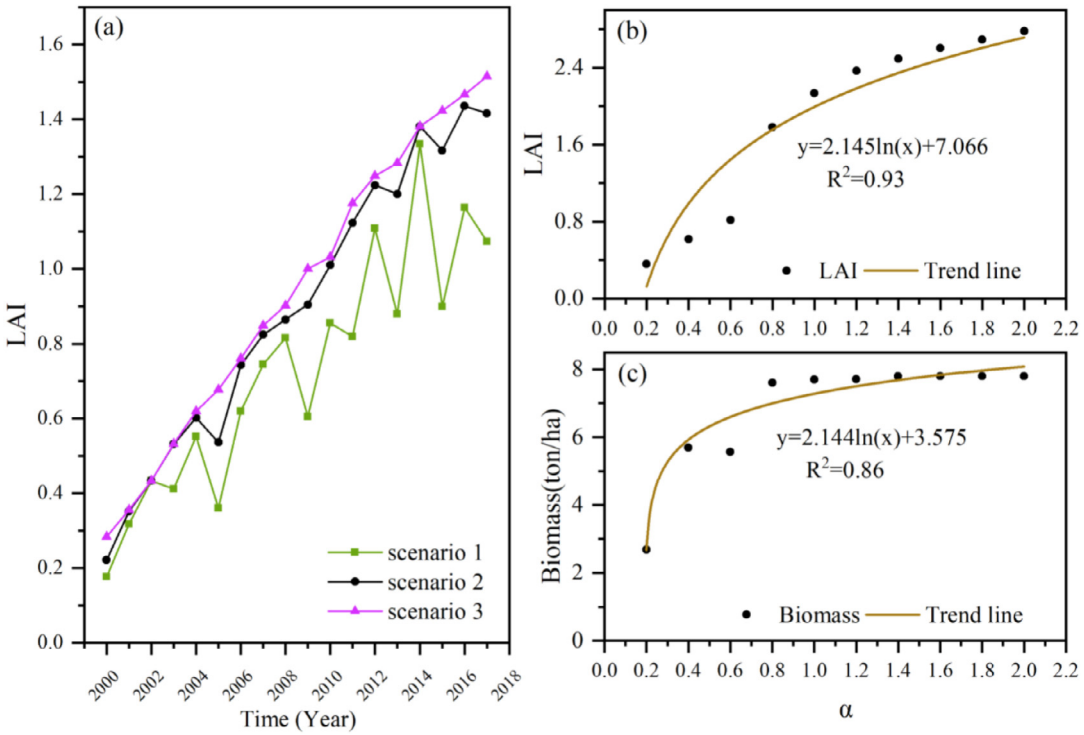

Fig. 9. (a) Changes in the leaf area index (LAI) in three scenarios from 2000–2017, and changes in (b) LAI and (c) biomass under different levels of precipitation. Note: α is the multiplier of precipitation.

growth. One is that the soil moisture memory is long-term. Mo et al. (2016) found that soil water storage during the previous non-growing season had a consistent spatial effect on the vegetation cover change in a semi-arid and semi-humid river basin, based on the annual water balance. Another reason is the nonlinear and delayed response of vegetation to precipitation change based on in-situ observations (Wolf et al., 2014). A further possible reason is the residence time of water flowing through different regions since it has been shown that there is a spatial phase difference between precipitation and NDVI dynamics (Helton et al., 2014; Mcdonnell and Beven, 2014).

4.2. Implications

Understanding the sensitivity of vegetation growth to precipitation change in afforestation areas is conducive to reasonably evaluating the environmental carrying capacity of the area and has implications for the selection and construction of afforestation areas. Taking the Loess Plateau as an example, there are distinct regional differences in precipitation changes (Miao et al., 2016; Sun et al., 2016; Wang et al., 2016; Yang et al., 2018), and drought has a certain impact on vegetation growth. Numerous studies have shown that vegetation restoration in the Loess Plateau leads to soil drought, which in turn affects the vegetation, resulting in the decline in vegetation coverage (Jia and Shao, 2014; Yang et al., 2014; Zhang et al., 2018; Su and Shangguan, 2019). Therefore, local climate conditions should be considered for further afforestation. In addition, in other afforestation areas around the world, such as Kubuqi Desert in Inner Mongolia, the Sahara, the Sahil in Africa, southwest Ireland, and the Mulde basin in Germany (Kemena et al., 2017; Lautenbach et al., 2017; Jovani-Sancho et al., 2018; Odoulami et al., 2018; Wang et al., 2018), vegetation growth may also be affected by precipitation, especially in arid areas, such as the Sahara (Kemena et al., 2017). These areas should be forested without affecting the ecological balance.

4.3. Uncertainties

There are uncertainties in this study. First, the uncertainties in the GLASS LAI may influence the model calibration. If additional ground LAI observations were to be used to further validate the model, the uncertainty would be reduced. Secondly, the model parameters would have introduced uncertainties in our attribution analysis (Galavi et al., 2019; Guo and Su, 2019; Yan et al., 2019; Zhang et al., 2019). Therefore, it would be advantageous to determine different vegetation parameters for various vegetation species across the Loess Plateau. Moreover, the model calibration and validation for the water balance were based on streamflow observations. Soil moisture evaluations are important to guarantee reasonable simulations for the water balance in vegetation growth. Thirdly, there are some small-scale water conservancy facilities in the study area, including small dams and scattered terraces (Guo, 2016). These water conservancy facilities affect hydrological processes and are more influential for runoff routing process than for runoff generation (which highly depends on soil water conditions). Our modelling did not specifically consider their impact. However, our model calibration attenuated the impact of the water conservancy facilities, as it ensured a reliable runoff simulation through parameter adjustment/optimization, so as to obtain acceptable simulations for the overall water balance. Moreover, this study focuses on vegetation growth processes, which are constrained by the soil moisture conditions after afforestation. The impact of terraces and check dams may, thus, not be significant.

5. Conclusions

This study employed a plant-water coupled ecohydrological model to simulate vegetation growth. The primary focus was to identify the sensitivity of vegetation growth to precipitation in a typical afforestation area on the Loess Plateau. After afforestation, the LAI increased from 0.34 in 2000 to 1.34 in 2017 in the study area, especially in the downstream areas with relatively sufficient water availability. We found that vegetation growth seems to have a logarithmic correlation

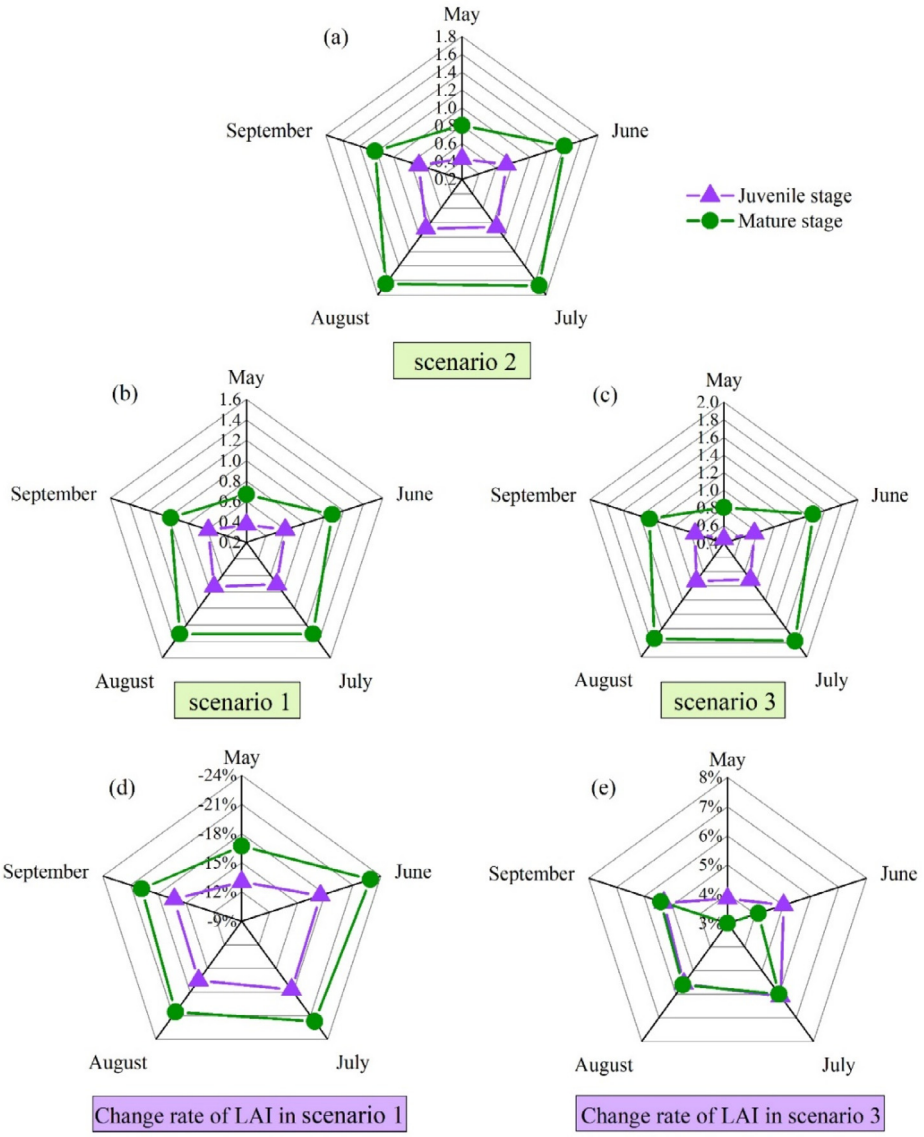

Fig. 10. (a) LAI simulation results of scenario 2 (actual precipitation); (b) LAI simulation results of scenario 1; (c) LAI simulation results of scenario 3; (d) LAI change rate of scenario 1 relative to scenario 2, and (e) LAI change rate of scenario 3 relative to scenario 2. (juvenile stage: 2000-2011, mature stages: 2012-2017.).

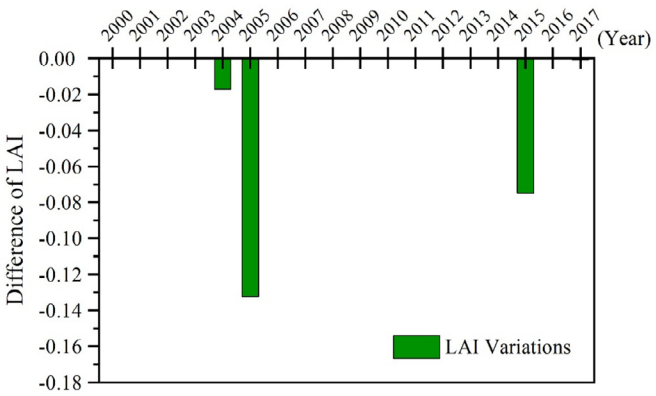

Fig. 11. Differences in the leaf area index (LAI) between scenarios 2 and 4 (scenario 2 – scenario 4).

with precipitation. The LAI and biomass were more sensitive to precipitation in the case of a low precipitation. Specifically, when the total precipitation was < 400 mm, the sensitivity of young vegetation to precipitation change was higher than that of mature vegetation. When the total precipitation was > 400 mm, on the contrary, the sensitivity of young vegetation to precipitation change was lower. In the juvenile stage, drought had a distinct lagged effect on vegetation growth, and can even affect vegetation growth in the following year, whereas in the mature stage, the lag effect from drought may be shorter. Although these findings are inferred from a small watershed, they are expected to not only contribute to the understanding of the hydrological and ecological processes of vegetation restoration but also provide reference values for the implementation of global afforestation projects and sustainable environmental management.

Declaration of Competing Interest

The authors declare that they have no known competing financial interests or personal relationships that could have appeared to influence the work reported in this paper. The authors declare the following financial interests/personal relationships which may be considered as potential competing interests.

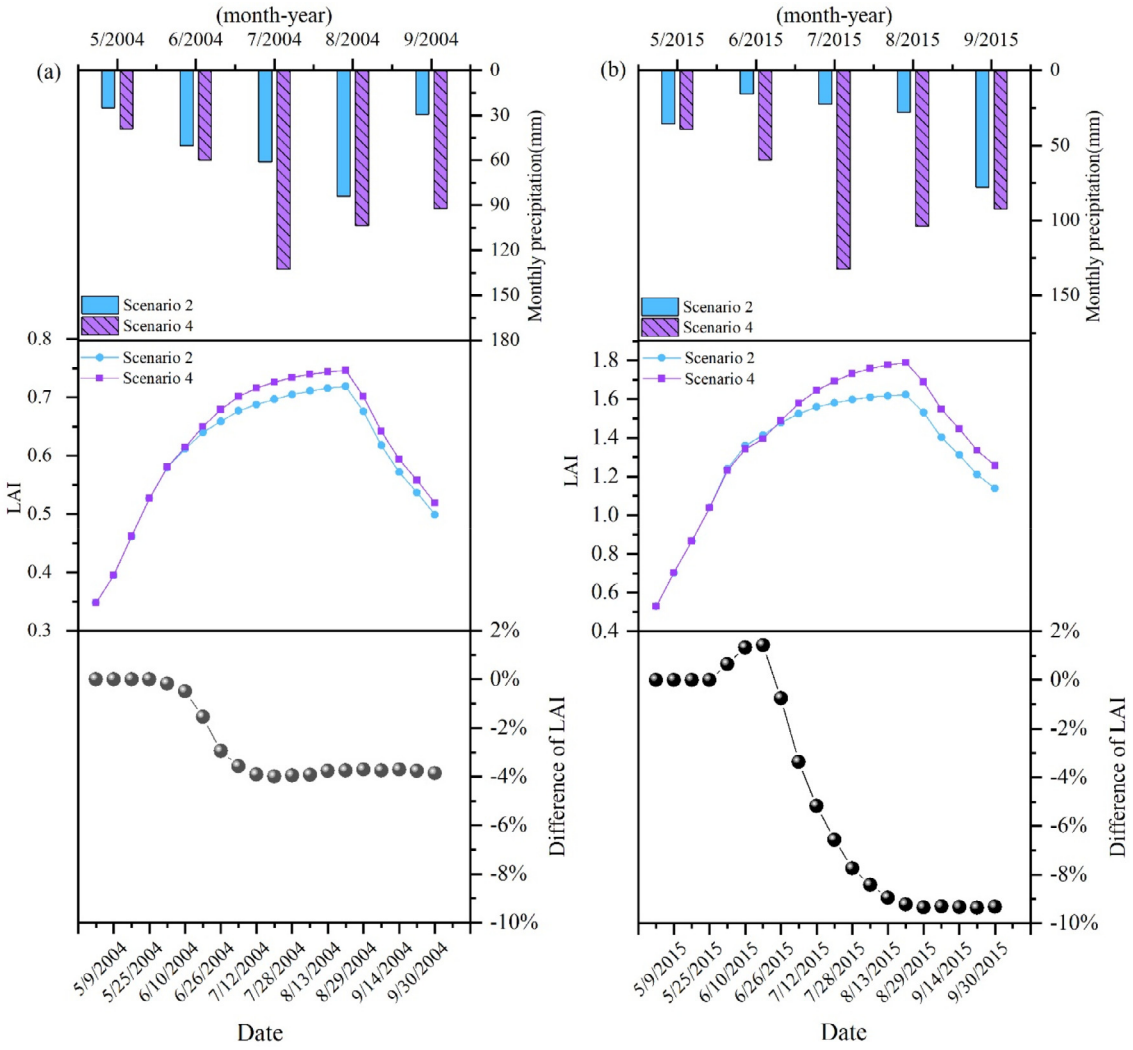

Fig. 12. Variations in the leaf area index (LAI) and precipitation in scenario 4 compared to scenario 2 from May to September in (a) 2004 and (b) 2015.

Acknowledgements

This research was supported by the National Natural Science Foundation of China (41971030) and the National Key Research and Development Program of China (NO.2016YFA0600103)

References

Arabi, M., Frankenberger, J.R., Engel, B.A., Arnold, J.G., 2008. Representation of agricultural conservation practices with SWAT. Hydrological Processes 22 (16), 3042–3055.

Arnold, J.G., Allen, P.M., Volk, M., Williams, J.R., Bosch, D.D., 2010. Assessment of Different Representations of Spatial Variability on Swat Model Performance. T Asabe 53 (5), 1433–1443.

Arnold, J.G., Moriasi, D.N., Gassman, P.W., Abbaspour, K.C., White, M.J., Srinivasan, R., Santhi, C., Harmel, R.D., van Griensven, A., Van Liew, M.W., Kannan, N., Jha, M.K., 2012. Swat: Model Use, Calibration, and Validation. T Asabe 55 (4), 1491–1508.

Arnold, J.G., Srinivasan, R., Muttiah, R.S., Allen, P.M., 1999. Continental Scale Simulation of the Hydrologic Balance. Journal of the American Water Resources Association 35 (5), 1037–1051.

Bonuma, N.B., Rossi, C.G., Arnold, J.G., Reichert, J.M., Paiva, E.M.C.D., 2013. Hydrology Evaluation of the Soil and Water Assessment Tool Considering Measurement Uncertainty for a Small Watershed in Southern Brazil. Appl Eng Agric 29 (2), 189–200.

Cao, M., Woodward, F.I., 1998. Dynamic responses of terrestrial ecosystem carbon cycling to global climate change. Nature 393 (6682), 249–252.

Chang, C.T., Wang, S.F., Vadeboncoeur, M.A., Lin, T.C., 2014. Relating vegetation dynamics to temperature and precipitation at monthly and annual timescales in Taiwan using MODIS vegetation indices. Int J Remote Sens 35 (2), 598–620.

Chen, C., He, B., Guo, L.L., Zhang, Y.F., Xie, X.M., Chen, Z.Y., 2018. Identifying Critical Climate Periods for Vegetation Growth in the Northern Hemisphere. Journal of Geophysical Research-Biogeosciences 123 (8), 2541–2552.

Chen, F., Weber, K.T., 2014. Assessing the impact of seasonal precipitation and temperature on vegetation in a grass-dominated rangeland. Rangeland J 36 (2), 185–190.

Chen, R.Y.X.Z.S.Y.H.2018. Estimating soil erosion response to land use/cover change in a catchment of the Loess Plateau, China Int Soil Water Conse Vol.6(No.1), 13-22.

Choi, Y.S., Jung, Y.H., Kim, J.H., Kim, K.-T., 2016. Soil Related Parameters Assessment Comparing Runoff Analysis using Harmonized World Soil Database (HWSD) and Detailed Soil Map. Journal of The Korean Society of Agricultural Engineers Vol 58 (No.4), 57–66.

Chu, H., Venevsky, S., Wu, C., Wang, M., 2019. NDVI-based vegetation dynamics and its response to climate changes at Amur-Heilongjiang River Basin from 1982 to 2015. Sci Total Environ 650 (Pt 2), 2051–2062.

Cramer, M.D., Hoffman, M.T., 2015. The Consequences of Precipitation Seasonality for Mediterranean-Ecosystem Vegetation of South Africa. Plos One 10 (12).

Del-Toro-Guerrero, F.J., Kretzschmar, T., Bullock, S.H., 2019. Precipitation and topography modulate vegetation greenness in the mountains of Baja California, Mexico. Int J Biometeorol 63 (10), 1425–1435.

Feng, X., Fu, B., Piao, S., Wang, S., Ciais, P., Zeng, Z., Lü, Y., Zeng, Y., Li, Y., Jiang, X., Wu, B., 2016. Revegetation in China's Loess Plateau is approaching sustainable water resource limits. Nature Climate Change 6 (11), 1019–1022.

Galavi, H., Kamal, M.R., Mirzaei, M., Ebrahimian, M., 2019. Assessing the contribution of different uncertainty sources in streamflow projections. Theoretical and Applied Climatology 137 (1-2), 1289–1303.

Gassman, P.W., Reyes, M.R., Green, C.H., Arnold, J.G., 2007. The soil and water assessment tool: Historical development, applications, and future research directions. Transactions of the Asabe 50 (4), 1211–1250.

Gaughan, A.E., Stevens, F.R., Gibbes, C., Southworth, J., Binford, M.W., 2012. Linking vegetation response to seasonal precipitation in the Okavango-Kwando-Zambezi catchment of southern Africa. Int J Remote Sens 33 (21), 6783–6804.

Gavito, M.E., Curtis, P.S., Mikkelsen, T.N., Jakobsen, I., 2001. Interactive effects of soil temperature, atmospheric carbon dioxide and soil N on root development, biomass and nutrient uptake of winter wheat during vegetative growth. J Exp Bot 52 (362),

1913–1923.
Green, J.K., Konings, A.G., Alemohammad, S.H., Berry, J., Entekhabi, D., Kolassa, J., Lee, J.-E., Gentine, P., 2017. Regionally strong feedbacks between the atmosphere and terrestrial biosphere %J Nature Geoscience. Nature Geoscience Vol.10 (No.6), 410–414.
Guo, J., Su, X.L., 2019. Parameter sensitivity analysis of SWAT model for streamflow simulation with multisource precipitation datasets. Hydrology Research 50 (3), 861–877.
Guo, X., 2016. Current situation and development direction of construction and management of small-scale water conservancy projects in Zichang County. Scientific and Technological Innovation and Application No.31, 225.
Helton, A.M., Poole, G.C., Payn, R.A., Izurieta, C., Stanford, J.A., 2014. Relative influences of the river channel, floodplain surface, and alluvial aquifer on simulated hydrologic residence time in a montane river floodplain. Geomorphology 205, 17–26.
Hu, Y., Tao, J., Xin, M., Wei, L., 1992. Study on the maturity of Shelterbelts in the Loess Plateau of East Gansu. FOREST SCIENCE AND TECHNOLOGY NO.5, 1–3.
Jia, X., Shao, M., Zhu, Y., Luo, Y., 2017. Soil moisture decline due to afforestation across the Loess Plateau, China. Journal of Hydrology Vol.546, 113–122.
Jia, Y.-H., Shao, M.-A., 2014. Dynamics of deep soil moisture in response to vegetational restoration on the Loess Plateau of China. Journal of Hydrology 519, 523–531.
Jiang, L., Guli, J., Bao, A., Guo, H., Ndayisaba, F., 2017. Vegetation dynamics and responses to climate change and human activities in Central Asia. Sci Total Environ 599-600, 967–980.
Jovani-Sancho, A.J., Cummins, T., Byrne, K.A., 2018. Soil respiration partitioning in afforested temperate peatlands. Biogeochemistry 141 (1), 1–21.
Justine, M.F., Yang, W.Q., Wu, F.Z., Khan, M.N., 2017. Dynamics of biomass and carbon sequestration across a chronosequence of masson pine plantations. J Geophys Res-Biogeo 122 (3), 578–591.
Juvany, M., Müller, M., Munné-Bosch, S., 2013. Plant age-related changes in cytokinins, leaf growth and pigment accumulation in juvenile mastic trees. Environmental and Experimental Botany 87, 10–18.
Kemena, T.P., Matthes, K., Martin, T., Wahl, S., Oschlies, A., 2017. Atmospheric feedbacks in North Africa from an irrigated, afforested Sahara. Climate Dynamics 50 (11-12), 4561–4581.
Kong, D., Zhang, Q., Singh, V.P., Shi, P., 2017. Seasonal vegetation response to climate change in the Northern Hemisphere (1982–2013). Global and Planetary Change 148, 1–8.
Krysanova, V., White, M., 2015. Advances in water resources assessment with SWAT—an overview. Hydrological Sciences Journal Vol. 60 (No.5), 1–13.
Lautenbach, S., Jungandreas, A., Blanke, J., Lehsten, V., Mühlner, S., Kühn, I., Volk, M., 2017. Trade-offs between plant species richness and carbon storage in the context of afforestation – Examples from afforestation scenarios in the Mulde Basin, Germany. Ecological Indicators 73, 139–155.
Li, L., Tsunekawa, A., Tsubo, M., Koike, A., Wang, J., 2010. Efficiency and its determinant factors for smallholder farms in the Grain for Green Program on the Loess Plateau, China. Journal of Food, Agriculture and Environment Vol.8 (No.3-4), 772–778.
Li, W.H.L, 2016. Driving force and changing trends of vegetation phenology in the Loess Plateau of China from 2000 to 2010. J Mt Sci-Engl 13 (NO. 5), 844–856.
Li, W.T., Du, J.K., Li, S.F., Zhou, X.B., Duan, Z., Li, R.J., Wang, S.Y.W.S.S., Li, M., 2019. The variation of vegetation productivity and its relationship to temperature and precipitation based on the GLASS-LAI of different African ecosystems from 1982 to 2013. Int J Biometeorol 63 (7), 847–860.
Liu, D.Y., Yang, L.Q., Jia, K., Liang, S.L., Xiao, Z.Q., Wei, X.Q., Yao, Y.J., Xia, M., Li, Y.W., 2018. Global Fractional Vegetation Cover Estimation Algorithm for VIIRS Reflectance Data Based on Machine Learning Methods. Remote Sens-Basel 10 (10).
Liu, F., 1998. Management technology of Hippophae rhamnoides soil and water conservation forest on the Loess Plateau. Shelterbelt Technology NO.1, 48–49.
Liu, J.Y., Zhang, Z.X., Xu, X.L., Kuang, W.H., Zhou, W.C., Zhang, S.W., Li, R.D., Yan, C.Z., Yu, D.S., Wu, S.X., Nan, J., 2010. Spatial patterns and driving forces of land use change in China during the early 21st century. J Geogr Sci 20 (4), 483–494.
Martiny, N., Camberlin, P., Richard, Y., Philippon, N., 2006. Compared regimes of NDVI and rainfall in semi-arid regions of Africa. International Journal of Remote Sensing 27 (23-24), 5201–5223.
Mberego, S., 2017. Temporal patterns of precipitation and vegetation variability over Botswana during extreme dry and wet rainfall seasons. Int J Climatol 37 (6), 2947–2960.
McDonnell, J.J., Beven, K., 2014. Debates-The future of hydrological sciences: A (common) path forward? A call to action aimed at understanding velocities, celerities and residence time distributions of the headwater hydrograph. Water Resources Research 50 (6), 5342–5350.
Miao, C., Sun, Q., Duan, Q., Wang, Y., 2016. Joint analysis of changes in temperature and precipitation on the Loess Plateau during the period 1961–2011. Climate Dynamics 47 (9-10), 3221–3234.
Mo, K.L., Chen, Q.W., Chen, C., Zhang, J.Y., Wang, L., Bao, Z.X., 2019. Spatiotemporal variation of correlation between vegetation cover and precipitation in an arid mountain-oasis river basin in northwest China. Journal of Hydrology 574, 138–147.
Muleta, M.K., Nicklow, J.W., 2005. Sensitivity and uncertainty analysis coupled with automatic calibration for a distributed watershed model. Journal of Hydrology 306 (1-4), 127–145.
Nachtergaele, F.O., Velthuizen, v.H., Verelst, L., Wiberg, D., Batjes, N.H., Dijkshoorn, J.A., Engelen, v.V.W.P., Fischer, G., Jones, A., Montanarella, L., Petri, M., Prieler, S., Teixeira, E., Shi, X., Jones, P., Thornton, P., 2012. Harmonized World Soil Database (version 1.2). Agricultural Systems Vol.139, 93–99.
Nash, J.E., Sutcliffe, J.V., 1970. River flow forecasting through conceptual models part I — A discussion of principles. Journal of Hydrology 10 (3), 282–290.
Nemani, R.R., Keeling, C.D., Hashimoto, H., Jolly, W.M., Piper, S.C., Tucker, C.J., Myneni, R.B., Running, S.W., 2003. Climate-Driven Increases in Global Terrestrial Net Primary Production from 1982 to 1999 %. J Science. Science of the Total Environment.
Odoulami, R.C., Abiodun, B.J., Ajayi, A.E., 2018. Modelling the potential impacts of afforestation on extreme precipitation over West Africa. Climate Dynamics 52 (3-4), 2185–2198.
Papagiannopoulou, C., Miralles, D.G., Dorigo, W.A., Verhoest, N.E.C., Depoorter, M., Waegeman, W., 2017. Vegetation anomalies caused by antecedent precipitation in most of the world. Environmental Research Letters 12 (7).
Pielke, R.A., Sr, Avissar, R, Raupach, M, Dolman, A.J, Zeng, X, Denning, A.S., 2003. Interactions between the atmosphere and terrestrial ecosystems: influence on weather and climate. Global Change Biology 4 (5), 461–475.
Quetin, G.R., Swann, A.L.S., 2017. Empirically Derived Sensitivity of Vegetation to Climate across Global Gradients of Temperature and Precipitation. Journal of Climate 30 (15), 5835–5849.
Santhi, C., Arnold, J.G., Williams, J.R., Dugas, W.A., Srinivasan, R., Hauck, L.M., 2001. Validation of the Swat Model on a Large Rwer Basin with Point and Nonpoint Sources. Journal of the American Water Resources Association 37 (5), 1169–1188.
Shen, M., Tang, Y., Chen, J., Zhu, X., Zheng, Y., 2011. Influences of temperature and precipitation before the growing season on spring phenology in grasslands of the central and eastern Qinghai-Tibetan Plateau. Agricultural and Forest Meteorology 151 (12), 1711–1722.
Su, B., Shangguan, Z., 2019. Decline in soil moisture due to vegetation restoration on the Loess Plateau of China. Land Degradation & Development 30 (3), 290–299.
Sun, W., Mu, X., Song, X., Wu, D., Cheng, A., Qiu, B., 2016. Changes in extreme temperature and precipitation events in the Loess Plateau (China) during 1960–2013 under global warming. Atmospheric Research 168, 33–48.
Sun, W., Zhu, H., Guo, S., 2015. Soil organic carbon as a function of land use and topography on the Loess Plateau of China. Ecological Engineering Vol 83, 249–257.
Tan, M.L., Gassman, P.W., Srinivasan, R., Arnold, J.G., Yang, X.Y., 2019. A Review of SWAT Studies in Southeast Asia: Applications, Challenges and Future Directions. Water-Sui 11 (5).
Tang, Z.G., Ma, J.H., Peng, H.H., Wang, S.H., Wei, J.F., 2017. Spatiotemporal changes of vegetation and their responses to temperature and precipitation in upper Shiyang river basin. Adv Space Res 60 (5), 969–979.
Wang, H., Sun, F., Xia, J., Liu, W., 2017. Impact of LUCC on streamflow based on the SWAT model over the Wei River basin on the Loess Plateau in China. Hydrology and Earth System Sciences 21 (4), 1929–1945.
Wang, L., Lee, X., Schultz, N., Chen, S., Wei, Z., Fu, C., Gao, Y., Yang, Y., Lin, G., 2018. Response of Surface Temperature to Afforestation in the Kubuqi Desert, Inner Mongolia. Journal of Geophysical Research: Atmospheres 123 (2), 948–964.
Wang, Q.-x., Wang, M.-b., Fan, X.-h., Zhang, F., Zhu, S.-z, Zhao, T.-l, 2016. Trends of temperature and precipitation extremes in the Loess Plateau Region of China, 1961–2010. Theoretical and Applied Climatology 129 (3-4), 949–963.
Wei, Z., Yoshimura, K., Wang, L., Miralles, D.G., Jasechko, S., Lee, X., 2017. Revisiting the contribution of transpiration to global terrestrial evapotranspiration. Geophysical Research Letters 44 (6), 2792–2801.
Wolf, S., Eugster, W., Ammann, C., Hani, M., Zielis, S., Hiller, R., Stieger, J., Imer, D., Merbold, L., Buchmann, N., 2014. Contrasting response of grassland versus forest carbon and water fluxes to spring drought in Switzerland (vol 8, 035007, 2013). Environmental Research Letters 9 (8).
Workie, T.G., Debella, H.J., 2018. Climate change and its effects on vegetation phenology across ecoregions of Ethiopia %J Global Ecology and Conservation. Global Ecology and Conservation Vol.13.
Wu, M., Schurgers, G., Rummukainen, M., Smith, B., Samuelsson, P., Jansson, C., Siltberg, J., May, W., 2016. Vegetation–climate feedbacks modulate rainfall patterns in Africa under future climate change. Earth System Dynamics 7 (3), 627–647.
Wu, Z.T., Wu, J.J., He, B., Liu, J.H., Wang, Q.F., Zhang, H., Liu, Y., 2014. Drought Offset Ecological Restoration Program-Induced Increase in Vegetation Activity in the Beijing-Tianjin Sand Source Region, China. Environ Sci Technol 48 (20), 12108–12117.
Xiao, Z., Liang, S., Jiang, B., 2017. Evaluation of four long time-series global leaf area index products. Agricultural and Forest Meteorology 246, 218–230.
Xiao, Z., Liang, S., Wang, T., Jiang, B., 2016. Retrieval of Leaf Area Index (LAI) and Fraction of Absorbed Photosynthetically Active Radiation (FAPAR) from VIIRS Time-Series Data. Remote Sensing 8 (4).
Xie, B., Jia, X., Qin, Z., Shen, J., Chang, Q., 2015a. Vegetation dynamics and climate change on the Loess Plateau, China: 1982–2011. Regional Environmental Change 16 (6), 1583–1594.
Xie, X.H., Liang, S.L., Yao, Y.J., Jia, K., Meng, S.S., Li, J., 2015b. Detection and attribution of changes in hydrological cycle over the Three-North region of China: Climate change versus afforestation effect. Agr Forest Meteorol 203, 74–87.
Xu, J., Li, Q., Wang, W., Xun, S., 2003. Studies on the mature period and renewal age of protection of Pinus nigrum coastal forest. Forestry Science NO.2, 91–97.
Yan, X.M., Lu, W.X., An, Y.K., Chang, Z.B., 2019. Uncertainty analysis of parameters in non-point source pollution simulation: case study of the application of the Soil and Water Assessment Tool model to Yitong River watershed in northeast China. Water and Environment Journal 33 (3), 390–400.
Yang, L., Wei, W., Chen, L., Chen, W., Wang, J., 2014. Response of temporal variation of soil moisture to vegetation restoration in semi-arid Loess Plateau, China. Catena 115, 123–133.
Yang, Q., Zheng, J., Zhang, Y., Yang, X., Liu, Z., IEEE, 2015. Relationship between precipitation and vegetation growth status of the northern slope of Tianshan Mountains based on GF-1 imagery: a case study of Hutubi County in Xinjiang. In: China International Conference on Geoinformatics.
Yang, Y., Yin, Z., Shan, Z., Wei, Q., Li, B., Guo, Q., Wei, L., Wang, Q., Zhang, J., 2018. Spatial variability and temporal trends of precipitation over the Loess Plateau of

China: 1957-2013. In: MATEC Web of Conferences. 246. pp. 1120.
Yao, Y., Xie, X.H., Meng, S.S., Zhu, B.W., Zhang, K., Wang, Y.B., 2019. Extended Dependence of the Hydrological Regime on the Land Cover Change in the Three-North Region of China: An Evaluation under Future Climate Conditions. Remote Sens-Basel 11 (1).
Yu, X., Xie, X.H., Meng, S.S., 2017. Modeling the Responses of Water and Sediment Discharge to Climate Change in the Upper Yellow River Basin, China. J Hydrol Eng 22 (12).
Yu, Y., Wei, W., Chen, L., Feng, T., Daryanto, S., 2019. Quantifying the effects of precipitation, vegetation, and land preparation techniques on runoff and soil erosion in a Loess watershed of China. Sci Total Environ 652, 755–764.
Yuan, W., Piao, S., Qin, D., Dong, W., Xia, J., Lin, H., Chen, M., 2018. Influence of Vegetation Growth on the Enhanced Seasonality of Atmospheric CO2. Global Biogeochemical Cycles 32 (1), 32–41.
Yue, P., Zhang, Q., Zhang, L., Li, H.Y., Yang, Y., Zeng, J., Wang, S., 2019. Long-term variations in energy partitioning and evapotranspiration in a semiarid grassland in the Loess Plateau of China. Agr Forest Meteorol 278.
Zeng, Z., Piao, S., Li, L.Z.X., Wang, T., Ciais, P., Lian, X., Yang, Y., Mao, J., Shi, X., Myneni, R.B., 2018. Impact of Earth Greening on the Terrestrial Water Cycle. J Climate 31 (7), 2633–2650.
Zhang, L.F., Xue, B.L., Yan, Y.H., Wang, G.Q., Sun, W.C., Li, Z.J., Yu, J.S., Xie, G., Shi, H.J., 2019. Model Uncertainty Analysis Methods for Semi-Arid Watersheds with Different Characteristics: A Comparative SWAT Case Study. Water 11 (6).
Zhang, S., Yang, D., Yang, Y., Piao, S., Yang, H., Lei, H., Fu, B., 2018. Excessive Afforestation and Soil Drying on China's Loess Plateau. Journal of Geophysical Research: Biogeosciences 123 (3), 923–935.
Zhao, S.Y.M.M.-g.J., 2012. Vegetation cover change and its climate driving force in recent 30 years in Loess Plateau, China %J Journal of Earth Environment. Journal of Earth Environment Vol.3 (No.6), 1174–1182.
Zhou, H., Van Rompaey, A., Wang, J.a, 2009. Detecting the impact of the “Grain for Green” program on the mean annual vegetation cover in the Shaanxi province. China using SPOT-VGT NDVI data Land Use Policy Vol 26 (No.4), 954–960.
Zhu, J., Jiang, F., Fan, Z., Liu, T., 2004. Studies on the maturity and regeneration of soil and water conservation forest of Robinia pseudoacacia on the Loess Plateau. Journal of ecology NO.5, 1–6.
Zhu, L., Gong, H., Dai, Z., Xu, T., Su, X., 2015. An integrated assessment of the impact of precipitation and groundwater on vegetation growth in arid and semiarid areas. Environ Earth Sci Vol.74 (No.6), 5009–5021.
ZP, W., XZ, Z., YT, H., M, L., PL, S., JX, Z., B, N., 2018. Responses of normalized difference vegetation index (NDVI) to precipitation changes on the grassland of Tibetan Plateau from 2000 to 2015. The Journal Of Applied Ecology Vol.29 (No.1), 75–83.